DEUTSCHES ELEKTRONEN-SYNCHROTRON DESY

DESY SR-83-01
January 1983

A METHOD FOR THE QUANTITATIVE DETERMINATION OF SYNCHROTRON RADIATION X-RAY SPECTRA FOR ABSOLUTE XRF - TRACE ELEMENT DETECTION

by

G. Tolkiehn and W. Petersen

Inst. f. Anorganische und Angewandte Chemie, Universität Hamburg

ISSN 0723-7979

NOTKESTRASSE 85 · 2 HAMBURG 52

To be sure that your preprints are promptly included in the
HIGH ENERGY PHYSICS INDEX ,
send them to the following address (if possible by air mail) :

DESY
Bibliothek
Notkestrasse 85
2 Hamburg 52
Germany

DESY SR-83-01
January 1983

ISSN 0723-7979

A Method for the Quantitative Determination of Synchrotron Radiation X-Ray Spectra for Absolute XRF - Trace Element Detection

G. Tolkiehn and W. Petersen
Inst. f. Anorganische und Angewandte Chemie
Universität Hamburg, 2000 Hamburg, FRG

Abstract

In the X-ray energy range the principal calculability of the synchrotron radiation flux-density and polarisation spectra is limited in practice by the fact that the essential parameters of vertical electron beam cross-section and -divergence are not well known due to instabilities that can occur at higher stored currents. This difficulty in calculating absolute X-ray spectra from first principles can be overcome by a semi-empirical method: By a polarisation measurement over a large energy range, effective electron beam parameters can be defined that lead to reliable calculated X-ray flux-density and polarisation spectra. With these data experimental scattering spectra could be verified extremely well on an absolute scale over an energy range of 2 keV to 35 keV. This is a necessary premise for the development of a method of absolute mass determination from XRF - spectra with synchrotron radiation excitation.

to be published in : Nuclear Instruments & Methods

Introduction

The synchrotron radiation emitted by an assumed electron beam of zero cross-section and divergence in a storage ring has a well-known spectral and angular intensity and polarisation distribution. These angular distributions are centered in the direction of electron momentum and have half-widths of the order of 0.1 mrad in the X-ray energy range. In a real storage ring the electron beam itself has a finite spatial and angular density. Its angular half-width is usually also of the order 0.1 mrad and also the ratio of its spatial half-width (beam-diameter) to distance source to experiment is usually of this order in X-ray rings.

Therefore size and divergence of the electron beam have to be included into the calculation of synchrotron radiation X-ray flux density and polarisation. This applies especially for intensities in cases where large angle scattering in the orbit plane occurs, so that strong polarisation corrections have to be included due to the linear polarisation of the X-rays (scattering background in XRF-measurements, energy-dispersive scattering intensities).

Quantitative description of a storage ring X-ray source

In principle the source can be described as a density function in a phase-space with three spatial and three momentum dimensions. In most cases only small parts of the total electron orbit contribute to one experiment, and the radiation is emitted only into directions close to the tangents of the ideal orbit. Therefore, it is useful to define the coordinates given in Fig. 1 for the description of the source.

A simple calculation[2] shows that the time averaged effective SR-source is approximately homogeneous in the horizontal angular coordinate (x') and that only a short z-range contributes to the source, if - as usual - the experiment accepts only a few mrad of horizontal divergence. Therefore, the z-dependence of the source parameters can be neglected and the x'-dependence approximated as constant. The source can be described assuming Gaussian distributions in all remaining variables as[2]:

$$\frac{\partial^4 N}{\partial x \partial y \partial x' \partial y'} = \frac{C \cdot \beta_y \ln 2}{\pi\, y_o^2} \exp \left\{ -\ln 2 \cdot \left(\frac{y^2}{y_o^2} + \frac{(y' + y\,\alpha_y/\beta_y)^2}{(y_o/\beta_y)^2} \right) \right\}$$

$$\cdot \frac{\sqrt{\ln 2}}{\sqrt{\pi}\, x_o} \exp \left(-\ln 2 \cdot \frac{x^2}{x_o^2} \right) \qquad (1)$$

where x_o and y_o are the hwhm of the distribution at x' = 0 and y' = 0. α and β are electron optical parameters (see e.g. Green[3]), which result from the magnet lattice of the storage ring. The parameter α describes convergence or divergence of the electron beam depending on its sign similar to the covariance of y and y', whereas β can be viewed as determining the ratio of spatial to angular width of the vertical distribution. The values for x_o, α, β and y_o vary alongthe electron orbit. Obviously the horizontal variables give a simple intensity factor proportional to the horizontal width of the entrance slit and are therefore no longer discussed here.

This distribution (1) has to be convoluted over y' with the polarisation components of the photon emission probability. Programs for the emission probability are available at every SR-center[4].

The photon phase-space density can now be projected to the experiment in the distance z from the tangent point by

$$y_z = zy' + y$$

and integrated over the remaining variables y, y' in the limits of the entrance-slit system of the experiment to yield the photon flux into the experiment. This caclulation was done for a rectangular entrance slit of 0.5 mm height and 2 mm width at a distance of 34 m from the tangent point of DORIS (beam F1). A number of values for the vertical beam size $2y_o$ were used, as y_o is not well known at the interesting high values of stored current (50 to 100 mA) in DORIS[5]. The calculation was done for the two polarisation components and the resulting degrees of linear polarisation $P = (I_x - I_y) / (I_x + I_y)$ as functions of the photon energy shown in Fig. 2 as dotted lines.

The total photon fluxes $I_x + I_y$ behind a small slit and the vertically polarised components are shown in Fig. 3. The significant influence of the vertical beamsize $2y_o$ also on the total-flux-spectra is obvious. In order to get a measure of y_o, the following experiment was designed.

Measurement of the degree of linear polarisation

Using a circular aperture of 0.5 mm in diameter, a scattering experiment was done on a mixture of gaseous N_2 and Xe. The sample was contained in a sample chamber which is sketched in Fig. 4. The scattered and fluorescent (Xe K- and L-lines) X-rays were measured with a rotatable Ge-detector over the energy range of 2 to 40 keV in horizontal and vertical direction with 30 mrad fwhm collimation. The sample chamber was carefully aligned parallel to the beam and into the center of gravity of the original X-ray beam by He-ionisation chambers designed for this purpose.

Possible geometric effects that might degrade the intensity ratio between vertical and horizontal observation can be cancelled out by evaluating the (unpolarized) fluorescence radiation of the Xe-K lines and calculating

$$P_{exp} = \left(\frac{S_y F_x}{S_x F_y} - 1 \right) / \left(\frac{S_y F_x}{S_x F_y} + 1 \right)$$

where S are the scattering count-rates and F the fluorescence count-rates in the vertical and horizontal spectrum (y and x respectively). In our data sets, however, F_x and F_y only differ by less than one percent after live-time and beamcurrent correction, which indicates good alignment. Two original spectra are shown in Fig. 5. The smoothed resulting P_{exp} (E) is shown as solid line in Fig. 2. The accuracy of P_{exp} is estimated to be better than $\pm$ 1% in the energy range shown. It indicates a value of $2y_o$ = 1,5 mm $\pm$ 0.1 mm.

Test of the calculated semi-empirical flux and polarisation spectra by comparison with a scattering experiment

A scattering experiment on a 0.95 mg/cm^2 Kapton foil with scattering angle 90^o in the orbit plane was performed in He-atmosphere in the X-ray

fluorescence set-up for trace analysis experiments[6]. The beam passes through a Be window of 0.4 mm thickness, a 0.026 mm Al window, and 0.9 m of He-atmosphere onto the sample at 45° angle of incidence. The configuration is shown in Fig. 6. The scattered radiation was monitored with a 5.0 mm thick Si (Li) detector. The circular primary aperture positioned in a distance of 350 mm from the sample has 0.2 mm diameter and the detector aperture 4.0 mm in a distance of 35 mm from the sample. The detector window consisted of 0.047 mm Kapton plus 6 mm air and 0.05 mm Be.

Again the assembly was adjusted parallel to and into the center of the beam using the monitors shown in Fig. 6. Using the data shown in Figs. 2 and 3 one can now calculate the expected scattered count-rate per 100 mA stored current.

The total scattered intensity $I(E, 90^\circ)$ in x-direction ($\theta = 90^\circ$) was calculated in nonrelativistic approximation (photon energies $E \ll 511$ keV) as:

$$I(E, 90^\circ) = I_y(E) \frac{r_o^2}{r^2} \sum_{Z=1}^{100} \left(F_Z^2 (E, 90^\circ) + S_Z (E, 90^\circ)\right) \cdot q_Z \cdot \frac{L}{A_Z} \qquad (2)$$

where I_y is the incoming intensity, r_o is the classical electron radius, r the distance from sample to detector. F_Z is the atomic form factor and S_Z the inelastic scattering factor both taken from Ref. 7, a_Z the areal mass density and A_Z the atomic mass number of the scattering atom species with atomic number Z. L is Loschmidt's number. The sum (2) was evaluated for C, N and O.

After putting in aperture areas, absorption correction for the detector windows, efficiency correction for the detector and energy calibration, the count-rate per channel at 100 mA and 0% dead time was calculated.

Selfabsorption in the sample, the hydrogen-component of the Kapton, scattering due to the in-plane component I_x of the incoming beam and the Compton wavelength shift were neglected as small corrections.The structure factor of Kapton was ignored as it is not readily available, although its effect on the scattering count-rate reaches 10% (see Fig. 7).

Out of similar reasons the fluorescence of impurity traces in the foil and the detector background were ignored in the calculation.

Calculation and measurement agree extremely well within the mentioned restrictions as is shown in Fig. 7. The largest sources of error are the effective size of the primary aperture, and size and distance of the secondary aperture. The total experimental error is estimated to be smaller than 25%.

Discussion

The vertical shape, size and divergence of the electron beam, which are essential for photon flux and polarisation of synchrotron X-radiation behind small vertical slits, are not well known in the region of maximum stored current due to instabilities[5]. Although optical imaging of the DORIS source indicate a rather complicated double-structure[8] in the vertical dimension, the use of simple Gaussians for the spatial and angular electron distributions together with the concept of defining an effective vertical beam diameter by a polarisation measurement, yields reliable calculated spectra of flux density and linear polarisaion. The accuracy of these data was tested by absolute measurements of the scattered intensity off a Kapton foil. The results agree very well over the whole energy range within an estimated maximum error of 25%, which is mainly due to uncertainties in the geometry factors and may be further improved.

This result enables absolute mass determination from X-ray fluorescence and scattering spectra with synchrotron radiation. The dependence of the vertical beam diameter on the beam current and its transition to the well-known value in the "low current" limit is subject of further investigation.

Acknowledgment

The support of Dr. A.Knöchel is gratefully acknowledged. Thanks for helpful discussions are due to Dr. R. Zietz, Dr. B. Schönfeld and Dr. H. Nesemann. The technical support by the staff of the HASYLAB is also acknowledged. The work was financed by the Bundesministerium für Forschung und Technologie.

References

1. J. Schwinger, Proc. Nat. Acad. Sci. (USA) 40, 132 (1954)

2. P. Rabe, G. Tolkiehn and A. Werner, Nucl. Instr. and Methods 171, 329 (1980)

3. G.K. Green (1977), BNL Report 50595, National Technical Information Service, Springfield, V.A.

4. Here, a program of W. Graeff was used.

5. H. Nesemann, private communication.

6. A detailed description of this experiment will be submitted to Microchim. Acta.

7. J.H. Hubbel, W.M. Keigele, E.A. Briggs, R.T. Brown, D.T. Cromer and R.J. Howerton, J. Phys. Chem. Ref. Data 4, 471 (1975)

8. R. Zietz, unpublished results.

Figure Captions

Fig. 1: Coordinate system for the description of the DORIS source.

Fig. 2: Calculated (circles) degree of linear polarisation of DORIS-F1-X-ray beam with 1.5 mm vertical aperture centered in the orbit plane for different diameters $2y_o$ of the electron beam versus photon energy. The calculation was done for the electronbeam parameters E_e = 3.3 GeV, α = 0.08 and β = 8.0 m.
Full line: result of measurement (see section 3).

Fig. 3: Calculated total flux spectra in photons/eV/s (upper curves) and vertically polarized component (lower curves) through a 0.5 mm high and 2 mm wide slit centered in the orbit plane of DORIS at beam F1 in 34 m distance from the tangent point for different electron beam diameters $2y_o$. Other parameters as in Fig. 2.

Fig. 4: Sample chamber of polarisation measurement (drawing not to scale).

Fig. 5: Original spectra of N_2/Xe mixture normalized to stored electron current and livetime in x- and y-direction.

Fig. 6: Schematic view of the XRF-experiment.

Fig. 7: Calculated (circles) and experimental (solid line) scattered intensity from a Kapton polyimid film in beam F1.

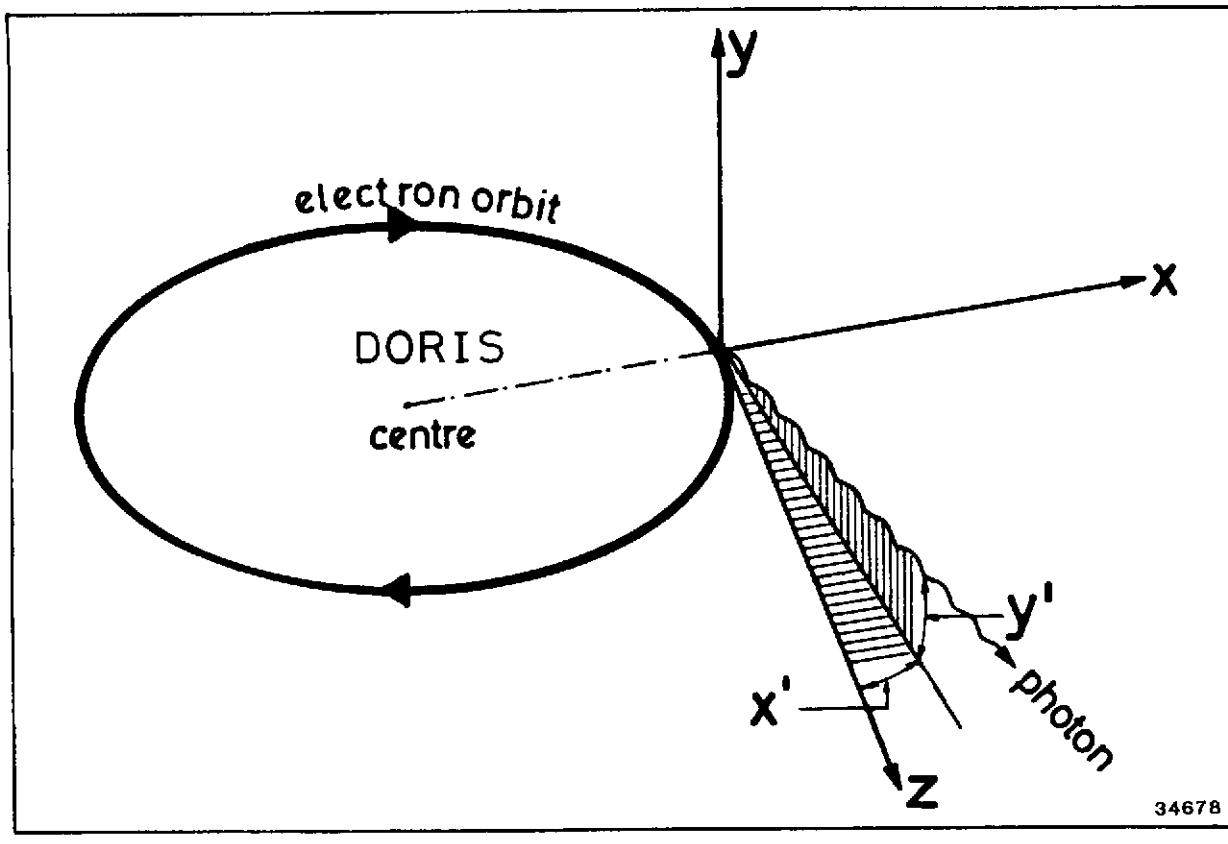
y
electron orbit
x
DORIS
centre
y'
photon
x'
z
34678

Fig. 1

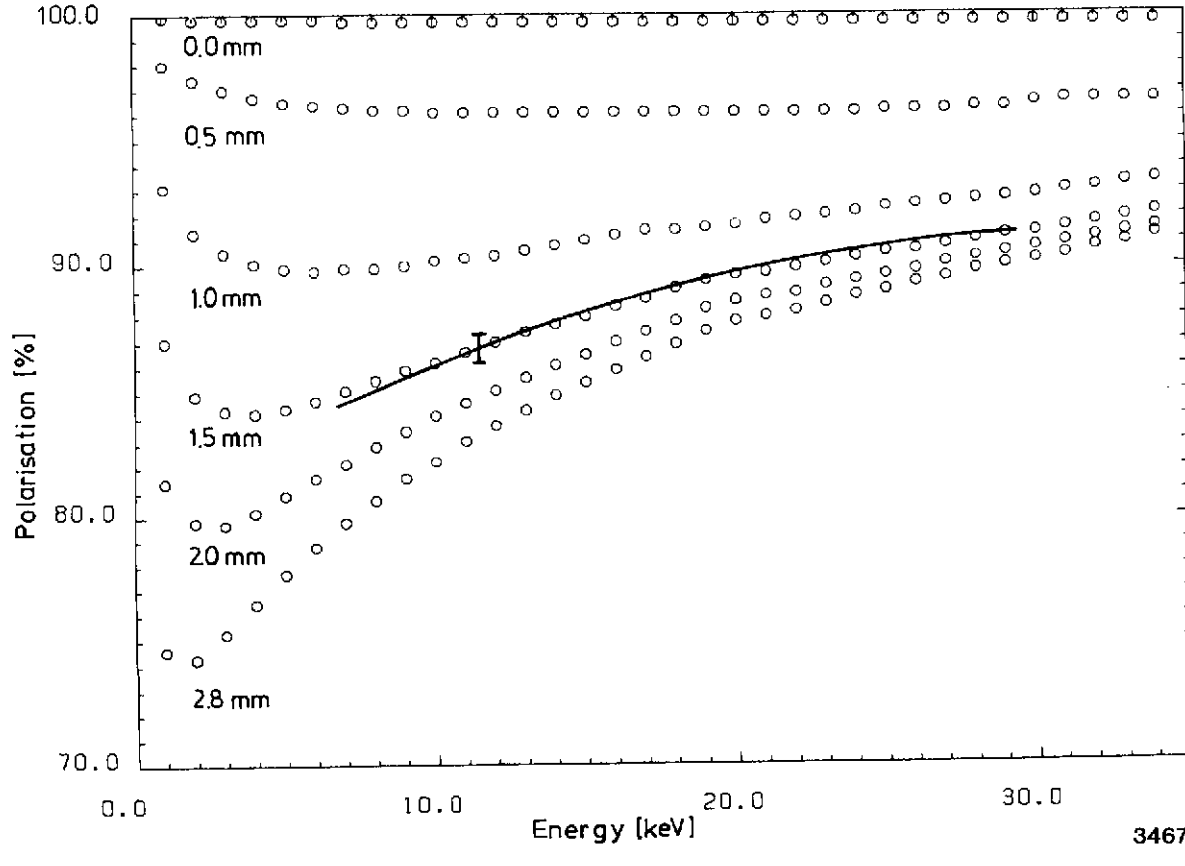
100.0
90.0
80.0
70.0
Polarisation [%]
0.0 mm
0.5 mm
1.0 mm
1.5 mm
2.0 mm
2.8 mm
0.0
10.0
20.0
30.0
Energy [keV]
34674

Fig. 2

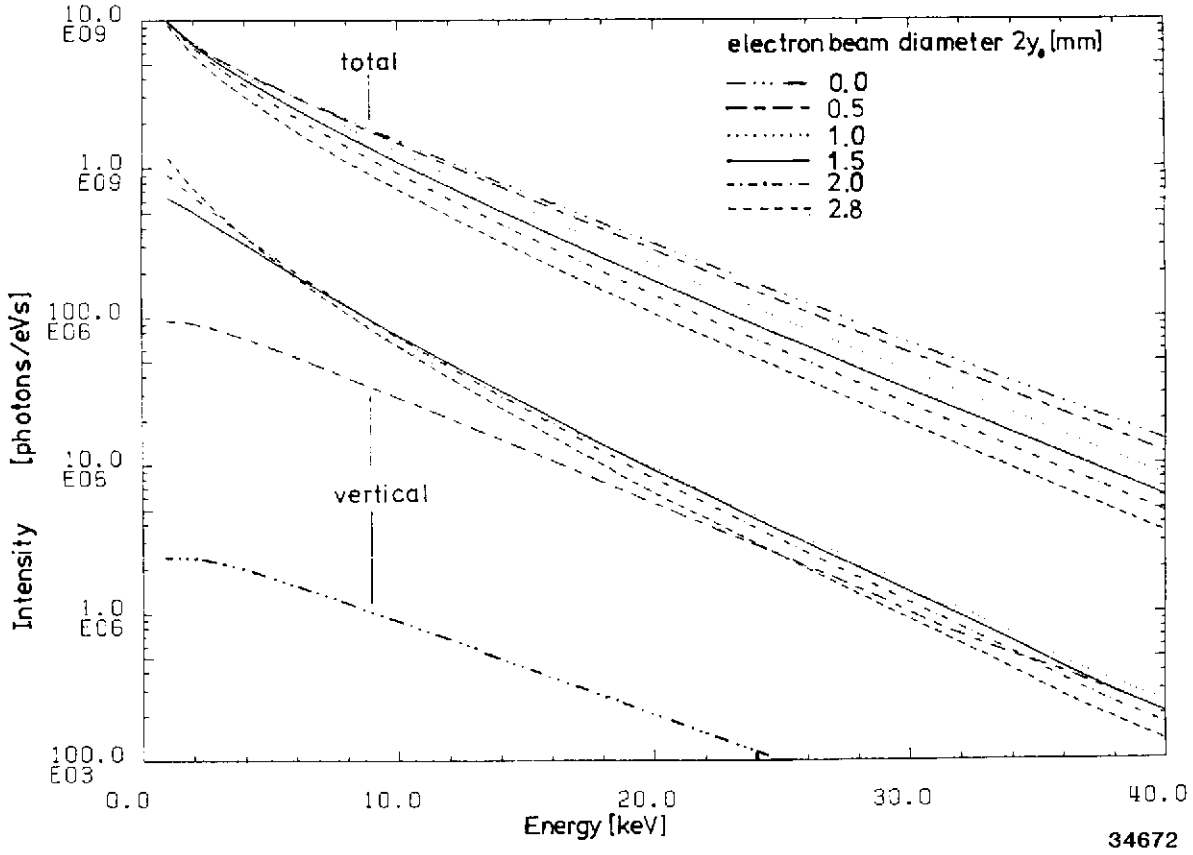
10.0 E09
1.0 E09
100.0 E06
10.0 E06
1.0 E06
100.0 E03
Intensity [photons/eVs]
total
vertical
electron beam diameter 2y0 [mm]
0.0
0.5
1.0
1.5
2.0
2.8
0.0
10.0
20.0
30.0
40.0
Energy [keV]
34672

Fig. 3

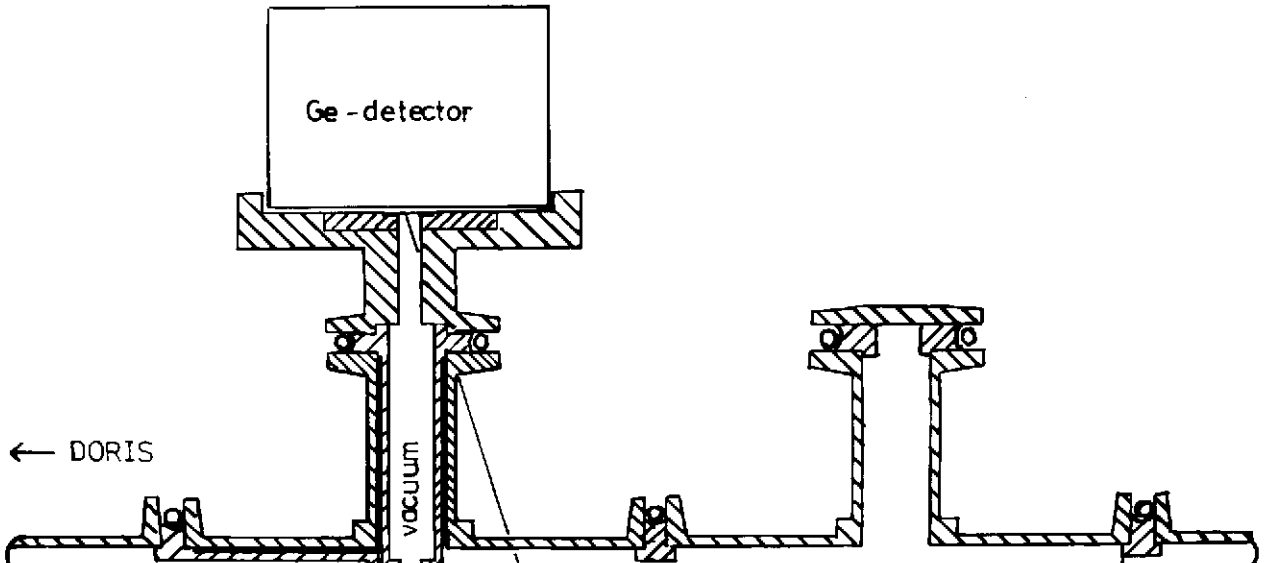
Ge - detector
← DORIS
vacuum
He
Xe/N2
He
Kapton-windows
34676

Fig. 4

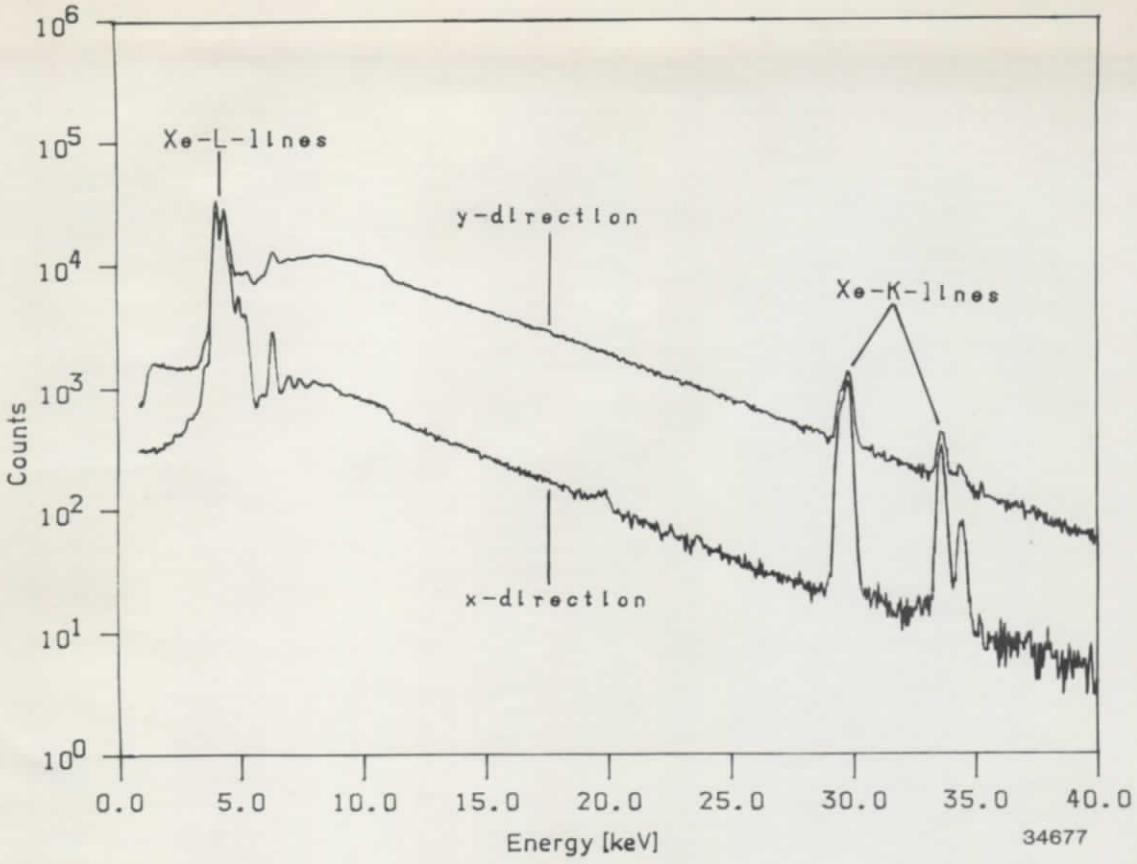
Xe-L-lines
y-direction
Xe-K-lines
x-direction
Counts
Energy [keV]
34677

Fig. 5

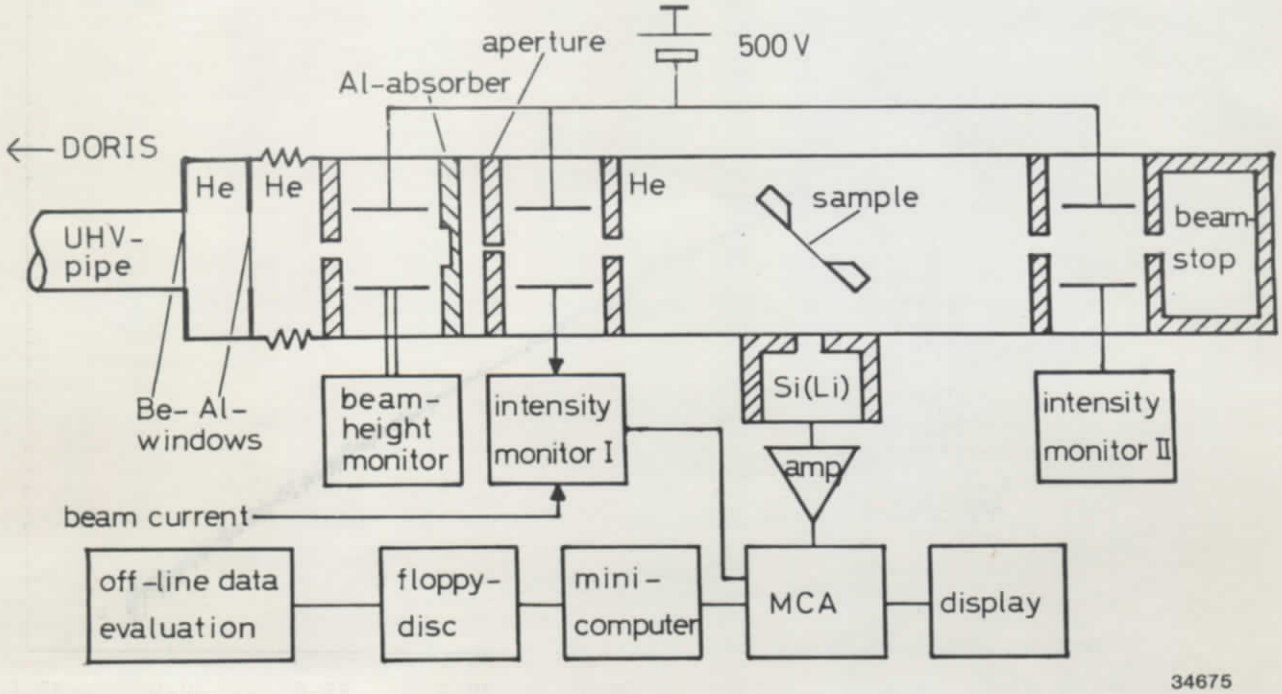
aperture
500 V
Al-absorber
DORIS
He
He
He
sample
beam-
stop
UHV-
pipe
Be- Al-
windows
beam-
height
monitor
intensity
monitor I
Si(Li)
amp
intensity
monitor II
beam current
off-line data
evaluation
floppy-
disc
mini-
computer
MCA
display
34675

Fig. 6

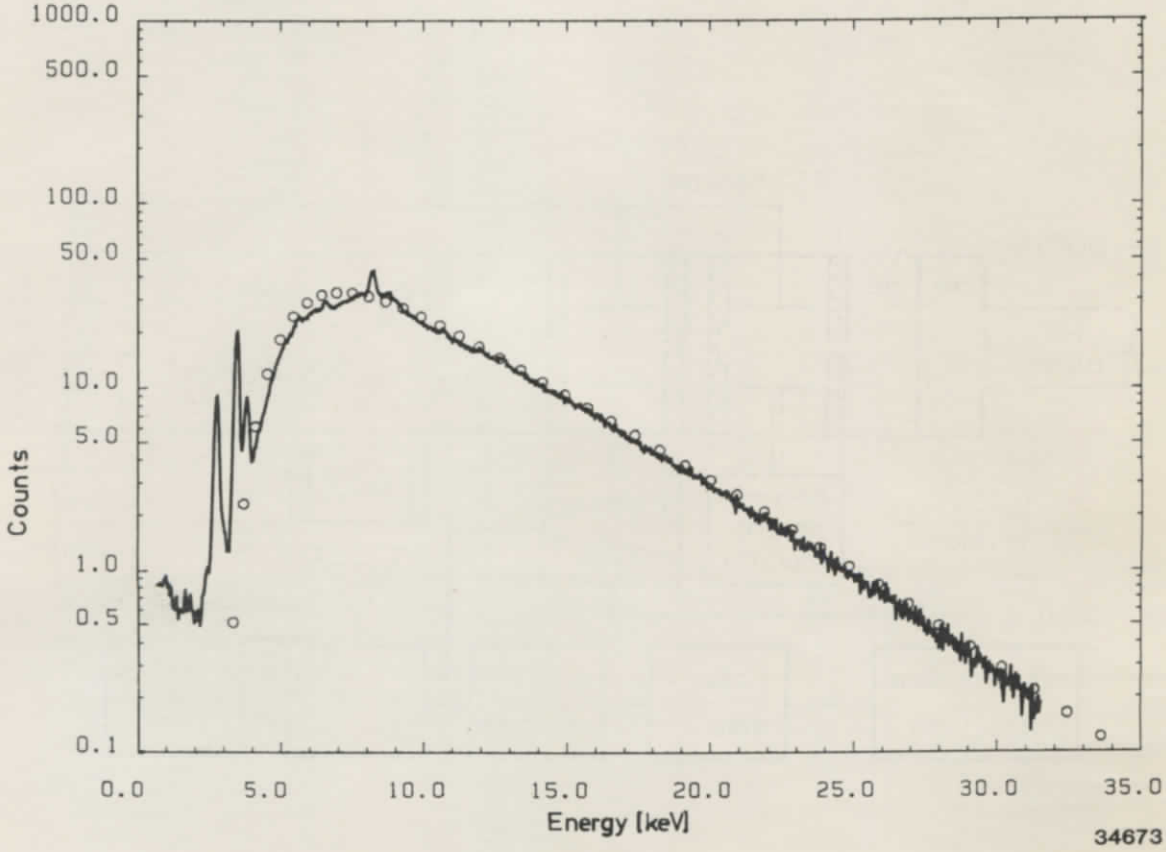
1000.0
500.0
100.0
50.0
10.0
5.0
1.0
0.5
0.1
Counts
0.0
5.0
10.0
15.0
20.0
25.0
30.0
35.0
Energy [keV]
34673

Fig. 7